

Circulating current in 1D Hubbard rings with long-range hopping: Comparison between exact diagonalization method and mean-field approach

Madhumita Saha^{1,*} and Santanu K. Maiti^{1,†}

¹*Physics and Applied Mathematics Unit, Indian Statistical Institute,
203 Barrackpore Trunk Road, Kolkata-700 108, India*

The interplay between Hubbard interaction, long-range hopping and disorder on persistent current in a mesoscopic one-dimensional conducting ring threaded by a magnetic flux ϕ is analyzed in detail. Two different methods, exact numerical diagonalization and Hartree-Fock mean field theory, are used to obtain numerical results from the many-body Hamiltonian. The current in a disordered ring gets enhanced as a result of electronic correlation and it becomes more significant when contributions from higher order hoppings, even if they are too small compared to nearest-neighbor hopping, are taken into account. Certainly this can be an interesting observation in the era of long-standing controversy between theoretical and experimental results of persistent current amplitudes. Along with these we also find half-flux quantum periodic current for some typical electron fillings and kink-like structures at different magnetic fluxes apart from $\phi = 0$ and $\pm\phi_0/2$. The scaling behavior of current is also discussed for the sake of completeness of our present analysis.

PACS numbers: 71.27.+a, 73.23.Ra, 73.23.-b

I. INTRODUCTION

The phenomenon of persistent current was first established during 1980's when Büttiker and his group have shown¹ that a small conducting ring carries a net circular current in presence of an Aharonov-Bohm (AB) flux ϕ , and it does not vanish even in presence of disorder. This is a pure quantum mechanical phase coherence phenomenon and a direct consequence of AB effect².

The experimental verification of it came after few years when Levy and co-workers did the pioneering experiment³ considering an ensemble of 10^7 independent Cu rings. Later several other experiments⁴⁻⁹ were carried out to confirm the existence of persistent current in different conducting loops. At the same time a substantial amount of theoretical work¹⁰⁻²² has also revealed several unique features along this direction. From the single ring measurement³ a period of ϕ_0 ($= ch/e$, the elementary flux-quantum) current has been observed, while some other experiments^{4,23} have shown both $\phi_0/2$ and ϕ_0 periodic currents. This half flux-quantum ($\phi_0/2$) periodic persistent current is not well explained from theoretical calculations and certainly it demands proper analysis. The another confliction between theoretical and experimental results is associated with the prediction of low-field currents, viz, slope of the current with flux ϕ in the limit $\phi \rightarrow 0$. Some experiments^{3,4} have shown diamagnetic (negative slope) nature, while paramagnetic (positive slope) response has been noticed from other experiments⁶. These observations do not really match well with theoretical observations. Many attempts have been made along this line and it has been observed that¹² the slope strongly depends on electronic filling, randomness, impurities, etc.

Finally, the most important controversy has been raised during the prediction of current amplitude. Only for nearly ballistic rings comparable currents are ob-

tained, while for diffusive rings the calculated current is much smaller and in some cases it is even less than two orders of magnitude compared to the experimental observations. In order to resolve this long-standing anomaly in diffusive rings, several attempts have been made considering the effects of different parameters. It has been verified that on-site Coulomb correlation plays a dominant role¹³⁻¹⁵ to enhance current amplitude in a disordered ring, though the enhancement is not sufficient to make it comparable to experimental observations. Later few theoretical models have been given considering the effect of higher order hopping integrals^{24,25} in addition to the usual nearest-neighbor hopping (NNH) in favor of current enhancement upto a certain level. So naturally the question comes how the current becomes affected if one includes the effect of both on-site Coulomb interaction and long-range hopping. This part has not been discussed so far, to the best of our knowledge.

In the present work we actually focus towards this direction. Here we consider interacting rings with higher-order hopping integrals and determine energy eigenvalues by *exact numerical diagonalization* of many-body tight-binding Hamiltonian. In this method we restrict ourselves to rings with few number of electrons, because of our computational limitations, as dimension of the matrix raises rapidly with ring size N and total number of electrons N_e . Different combinations of up and down spin electrons are taken into account and from our results we observe some similarities in current-flux characteristics for odd N_e as well as even N_e , which certainly help us to generalize the results for larger ring size with higher electrons. However, it is always good to have some definite results of large interacting rings to understand the interplay between long-range hopping, disorder and e-e interaction. We thus require an appropriate technique to work out such a many-body problem. Here we use Hartree-Fock (HF) mean-field theory²⁶⁻²⁹ to find energy eigenvalues and hence persistent currents, and, compare

these currents with exact numerical diagonalization analysis. Scrutinizing the results we show that persistent current behaves almost identical in these two methods, but one can miss some important signatures of current at some typical fluxes, particularly in the limit $\phi \rightarrow 0$. This is an artifact of the mean-field calculations.

Several interesting features are obtained from our calculations. The current gets enhanced in a disordered ring as a result of Coulomb repulsion and it becomes more effective when higher order hopping integrals are included. Under this situation current becomes quite comparable to that of a perfect ring. In addition we also discuss the appearance of half flux-quantum periodicity for some particular electron fillings and some kink-like structures at different fluxes apart from $\phi = 0$ and $\pm\phi_0/2$. Finally, scaling behavior of current is also discussed, for the sake of completeness.

The rest of the work is arranged as follows. In Sec. II we describe the ring model and theoretical procedure to construct the Hamiltonian matrix and calculation of persistent current as a function of flux ϕ . Later, in Sec. III we discuss numerical results, and finally, a brief summary is given in Sec. IV.

II. MODEL AND THEORETICAL FORMULATION

A. Model and Tight-Binding Hamiltonian

The schematic diagram of our model is illustrated in Fig. 1, where a mesoscopic ring is subjected to on-site Hubbard interaction and long-range hoppings, viz, second-neighbor hopping (SNH) and third-neighbor hopping (TNH) including nearest-neighbor hopping. Under the application of an AB flux ϕ , a net circulating current is established in the ring.

To describe this model we employ a tight-binding (TB) framework. For a N -site ring the TB Hamiltonian looks like,

$$\begin{aligned} \mathbf{H} = & \sum_{j,\sigma} \epsilon_j c_{j,\sigma}^\dagger c_{j,\sigma} + t \sum_{j,\sigma} \left[e^{i\theta_1} c_{j,\sigma}^\dagger c_{j+1,\sigma} \right. \\ & \left. + e^{-i\theta_1} c_{j+1,\sigma}^\dagger c_{j,\sigma} \right] \\ & + t_1 \sum_{j,\sigma} \left[e^{i\theta_2} c_{j,\sigma}^\dagger c_{j+2,\sigma} + e^{-i\theta_2} c_{j+2,\sigma}^\dagger c_{j,\sigma} \right] \\ & + t_2 \sum_{j,\sigma} \left[e^{i\theta_3} c_{j,\sigma}^\dagger c_{j+3,\sigma} + e^{-i\theta_3} c_{j+3,\sigma}^\dagger c_{j,\sigma} \right] \\ & + U \sum_j c_{j,\uparrow}^\dagger c_{j,\uparrow} c_{j,\downarrow}^\dagger c_{j,\downarrow} \end{aligned} \quad (1)$$

where ϵ_j gives the site energy for j th site and $c_{j,\sigma}^\dagger$ ($c_{j,\sigma}$) represents the creation (annihilation) operator. t describes the nearest-neighbor hopping strength and due to this hopping a phase factor θ_1 ($= 2\pi\phi/\phi_0$) is introduced

into the Hamiltonian. Similarly, t_1 and t_2 denote the SNH and TNH integrals, respectively, with the associated

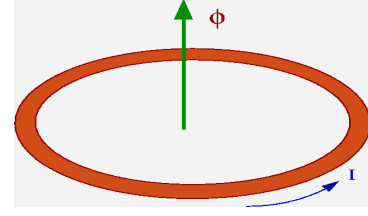


FIG. 1: (Color online). Schematic view of a mesoscopic ring threaded by an Aharonov-Bohm flux ϕ . A net circulating current I is established in the ring.

phase factors $\theta_2 = 2\theta_1$ and $\theta_3 = 3\theta_1$. The parameter U measures the Hubbard interaction strength. Setting $\epsilon_j = \text{constant } \forall j$ we get a perfect ring and without loss of generality we can fix it to zero, while for a disordered ring site energies are chosen *randomly* from a Box distribution function of width W .

B. Method I: Exact Numerical Diagonalization

Using the TB Hamiltonian, Eq. 1, we construct matrix elements through the prescription $\mathbf{H}_{mn} = \langle \psi_m | \mathbf{H} | \psi_n \rangle$, where $|\psi_m\rangle$ and $|\psi_n\rangle$ are basis states associated with total number of up (N_{up}) and down (N_{dn}) spin electrons in a ring. For example, for a ring with two opposite spin electrons (viz, $N_{up} = N_{dn} = 1$) the state vectors are like: $|\psi_m\rangle = c_{p\uparrow}^\dagger c_{q\downarrow}^\dagger |0\rangle$ and $|\psi_n\rangle = c_{k\uparrow}^\dagger c_{l\downarrow}^\dagger |0\rangle$, where $|0\rangle$ is the vacuum state. In a similar way, we can choose the basis states for any ring with different N_{up} and N_{dn} and construct the required many-body Hamiltonian matrix. Diagonalizing this matrix, we find energy eigenvalues and eventually determine persistent current at absolute zero temperature from the relation

$$I(\phi) = -\frac{\partial E_0(\phi)}{\partial \phi}, \quad (2)$$

where $E_0(\phi)$ is the ground state energy.

C. Method II: Hartree-Fock Mean-Field Approach

In this method the interacting Hamiltonian \mathbf{H} is decoupled into two non-interacting parts^{28,29}, say, \mathbf{H}_\uparrow and \mathbf{H}_\downarrow , associated with up and down spin electrons. Diagonalizing these non-interacting Hamiltonians (\mathbf{H}_\uparrow and \mathbf{H}_\downarrow), we find energy eigenvalues, and eventually, calculate the ground state energy at absolute zero temperature for a system containing N_{up} and N_{dn} spin electrons from the relation

$$E_0 = \sum_{n=1}^{N_{up}} E_{n\uparrow} + \sum_{n=1}^{N_{dn}} E_{n\downarrow} - \sum_{i=1}^N U \langle n_{i\uparrow} \rangle \langle n_{i\downarrow} \rangle \quad (3)$$

where $E_{n\sigma}$'s are the energy eigenvalues and $\langle n_{i\sigma} \rangle = \langle c_{i\sigma}^\dagger c_{i\sigma} \rangle$.

Finally, persistent current is determined from the relation given in Eq. 2.

III. RESULTS AND DISCUSSION

We present our results in two different sub-sections. In the first part (sub-section A) we determine persistent current by evaluating ground state energy from *exact numerical diagonalization* of many-body Hamiltonian. Starting from a ring with two opposite spin electrons we consider upto six-electron system. For a fixed $N_e (= N_{up} + N_{dn})$, different combinations of N_{up} and N_{dn} are taken into account to explore all the basic features of persistent current in interacting rings. While, in the other part (sub-section B), persistent current is found out by determining ground state energy from HF mean-field approach.

Throughout the analysis we set $t = -1$ eV (t_1 and t_2 are variable and they are mentioned in appropriate places) and all the energies are scaled with respect to it. The current is measured in unit of et/h .

A. Exact numerical diagonalization analysis

1. Impurity free rings

Let us first concentrate on interacting rings without any impurity i.e., $\epsilon_j = 0 \forall j$.

Case 1 - Ring with two electrons: To have an interacting ring with two electrons we consider one up and one down spin electron i.e., $N_{up} = N_{dn} = 1$. For this configuration we select basis states as $|\psi_m\rangle = c_{p\uparrow}^\dagger c_{q\downarrow}^\dagger |0\rangle$ and $|\psi_n\rangle = c_{k\uparrow}^\dagger c_{l\downarrow}^\dagger |0\rangle$ and the dimension of matrix becomes $N^2 \times N^2$ for a N -site ring.

Figure 2 displays the variation of ground state energy and corresponding persistent current with ϕ for a 10-site ring having two opposite spin electrons for different values of correlation strength U . In the 1st row the results are shown when the ring is described with only NNH integral, while in the 2nd row we add the effect of SNH integral and finally in the last row both SNH and TNH integrals are taken into account. The results are noteworthy. (i) The ground state energy exhibits U -independent energy region across $\phi = \pm\phi_0/2$ and the width of this region gets increased with increasing U , while it decreases with the inclusion of higher order hopping integrals, as clearly seen by comparing the E_0 - ϕ spectra given in Figs. 2(a), (c) and (e). This behavior is nicely reflected in current-flux characteristics yielding a kink-like structure. A sudden change in direction of current takes place as a result of this kink, and interestingly we see that inside a kink the slope of the current remains unchanged irrespective of U . (ii) For a fixed correlation strength U , the slope of E_0 -

ϕ curve gets increased with higher order hopping which results a larger current. Here it is important to note that though TNH strength is much weaker than SNH, it con-

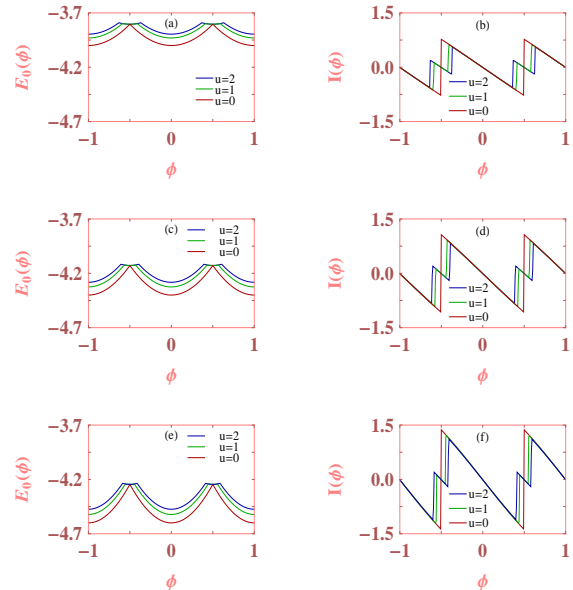


FIG. 2: (Color online). Dependence of ground state energy with flux ϕ and associated current for a 10-site ring with two opposite spin electrons for different values of U , where the 1st, 2nd and 3rd rows correspond to the ring with only NNH; NNH and SNH; and NNH, SNH and TNH integrals, respectively. Here we set $t_1 = -0.1$ and $t_2 = -0.05$.

tributes significantly to raise the current which is visible from the spectra given in Figs. 2(d) and (f). Certainly, more current is expected in presence of additional higher order hopping, beyond TNH, though their strengths are vanishingly small. Physically this is easily understandable since the incorporation of additional hopping allows electrons to hop further and thereby increases electronic current. (iii) A reduction of current is observed with increasing U when all the other physical parameters describing the system remain unchanged. This is solely due to the repulsive nature of electron-electron (e-e) interaction. It suggests that lesser and lesser current is expected with increasing U , though it eventually reaches to a finite value (not shown here) and never drops to zero since $N_e < N$, which we verify through our detailed numerical analysis.

To have a deeper insight about the role of SNH and TNH integrals in Fig. 3 we present the variation of ground state energy along with persistent current as a function of ϕ considering $U = 1$ for the same ring size as taken in Fig. 2 for some typical values of t_1 and t_2 . From the spectra given in 1st row we see that with increasing t_1 current gets enhanced following energy-flux diagram but it (t_1) reduces the kink size. Further enhancement of current can be also made possible with the inclusion of TNH (see Fig. 3(d)), and like t_1 , t_2 is also responsible for the reduction of kink size, though these kinks do not

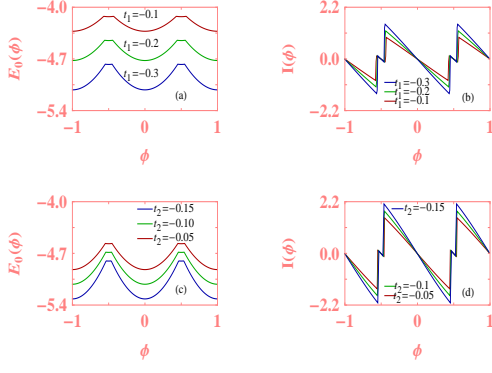


FIG. 3: (Color online). Variation of ground state energy and corresponding current as function of ϕ for a 10-site ring with two opposite spin electrons considering $U = 1$ for different values of t_1 and t_2 . For the 1st row the ring is described with NNH and SNH, while in the 2nd row the effect of TNH is also included where t_1 is fixed at -0.2 .

vanish even for larger t_1 and t_2 as long as e-e interaction is there. For this two-spin system we get only ϕ_0 periodic current.

Case 2 - Ring with three electrons: Now we consider a ring with one down spin and two up spin electrons to have a three-electron ring system, and here we choose $|\psi_1\rangle = c_{p\uparrow}^\dagger c_{q\uparrow}^\dagger c_{r\downarrow}^\dagger |0\rangle$ and $|\psi_2\rangle = c_{k\uparrow}^\dagger c_{l\uparrow}^\dagger c_{m\downarrow}^\dagger |0\rangle$. With this configuration the dimension of the matrix for a N -site ring becomes: $N^2(N-1)/2 \times N^2(N-1)/2$. Two different cases are analyzed depending on the filling factor those are as follows.

- **Half-filled ring:** In Fig. 4 we present the variation of ground state energy E_0 and its corresponding persistent current as a function of AB flux ϕ in the half-filled limit

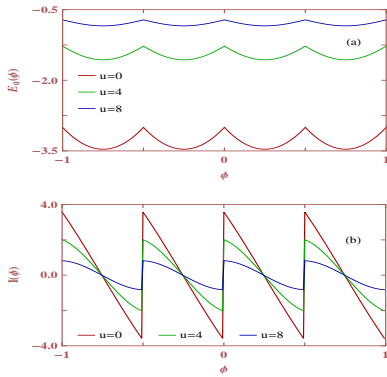


FIG. 4: (Color online). E_0 - ϕ and corresponding I - ϕ characteristics of a 3-electron ($N_{up} = 2$ and $N_{dn} = 1$) system in the half-filled limit (viz, $N = 3$). Here SNH and TNH are not applicable.

for three typical values of U . Two important features are observed. (i) Ground state energy exhibits half-flux-quantum ($\phi_0/2$) periodicity with ϕ , and it is nicely re-

flected in the current-flux characteristics. To illustrate this fact we can set the interaction strength U to zero, since it does not affect $\phi_0/2$ periodicity (which is shown from the E_0 - ϕ and I - ϕ spectra). Due to this simplification we can handle the problem very easily as it becomes

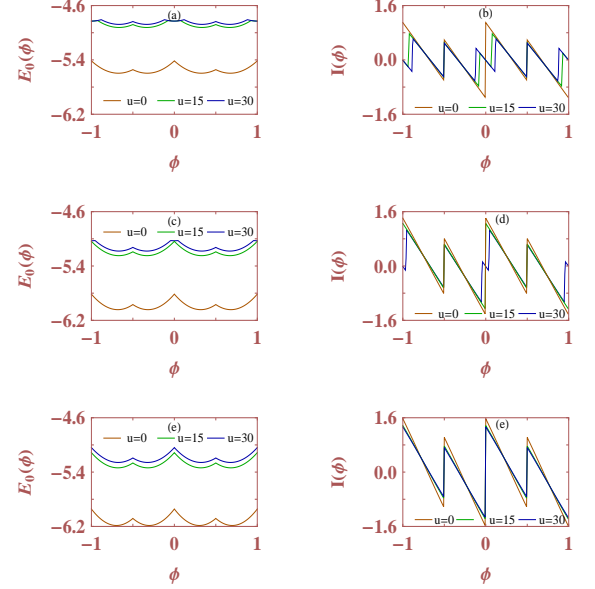


FIG. 5: (Color online). E_0 - ϕ and I - ϕ curves for a 8-site ring with three electrons ($N_{up} = 2$, $N_{dn} = 1$), where the first, second and third rows correspond to the ring with only NNH; NNH and SNH; NNH, SNH and TNH integrals, respectively. The other parameters are: $t_1 = -0.1$ and $t_2 = -0.05$.

now a non-interacting one. For $N = 3$, three energy eigenstates are obtained where each of these states can have maximum two opposite spin electrons. Therefore, ground state energy is obtained by placing two opposite spin electrons in the lowest non-interacting energy level and the third electron (up spin) in the first excited level. Quite interestingly, we observe that all such distinct energy levels have ϕ_0 flux-quantum periodicity. But as long as the highest accessible energy level (here it is 1st excited state) contains a *single electron*, instead of two, the net ground state energy of the system gets strange $\phi_0/2$ periodicity. This peculiar $\phi_0/2$ periodicity also remains unchanged even in presence of U , which we claim from our results. (ii) No kink-like structure appears in I - ϕ curves which implies that at half-filling no U -independent state contributes to the lowest energy for any flux window.

For such filling, current decreases rapidly with the correlation strength U , as there is no empty site.

- **Non-half-filled ring:** The results of a three-electron non-half-filled ring ($N = 8$) are shown in Fig. 5 which exhibit some interesting patterns unlike the half-filled case. (i) From the spectra it is shown that the $\phi_0/2$ periodicity disappears and the current, associated with ground state energy, regains its usual ϕ_0 periodicity. (ii) The kink-like structure, associated with U -independent states, appears

in persistent current across $\phi = 0$ at sufficiently large value of U , and the width of such kink decreases with the inclusion of higher order hopping integrals like SNH and TNH. In this context it is important to note that for two-electron case, kink appears as long as the interaction is turned on. The other features viz, the reduction of current with U and its enhancement with higher order hopping integrals remain same as discussed in a two-electron ring system.

Case 3 - Ring with four electrons: For four-electron system we consider two distinct configurations depending on N_{up} and N_{dn} . In one configuration we set $N_{up} = 3$ and $N_{dn} = 1$, while for the other we choose $N_{up} = N_{dn} = 2$.

■ **Configuration I – Ring with $N_{up} = 3$ and $N_{dn} = 1$:** The dimension of the Hamiltonian matrix for this setup becomes $(N^2/6)(N-1)(N-2) \times (N^2/6)(N-1)(N-2)$, where the basis states are: $|\psi_1\rangle = c_{p\uparrow}^\dagger c_{q\uparrow}^\dagger c_{r\uparrow}^\dagger c_{s\downarrow}^\dagger |0\rangle$ and $|\psi_2\rangle = c_{k\uparrow}^\dagger c_{l\uparrow}^\dagger c_{m\uparrow}^\dagger c_{n\downarrow}^\dagger |0\rangle$.

The characteristics features of ground state energy and corresponding current for a half-filled ring with four electrons ($N_{up} = 3$ and $N_{dn} = 1$) are shown in Fig. 6. At $U = 0$, a sharp transition occurs in persistent current

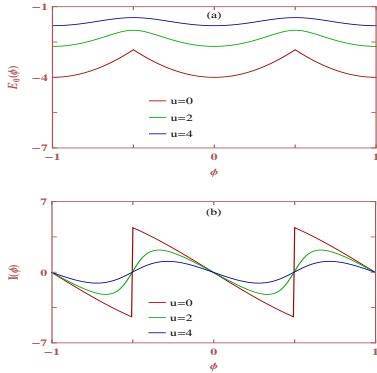


FIG. 6: (Color online). E_0 - ϕ and I - ϕ curves of a four-site ring ($N = 4$) with $N_e = 4$ ($N_{up} = 3$ and $N_{dn} = 1$) for different values of U considering NNH only.

around $\phi = \pm\phi_0/2$, while for finite U the current gets reduced and varies continuously with ϕ . This continuous-like variation is not quite trivial as obtained in traditional disordered case. While, the reduction of current with U is anticipated easily for this half-filled case.

Away from half-filling some kink-like structures are visible in I - ϕ spectra reflecting the E_0 - ϕ curves, and the most crucial point is that these kinks are generated as a result of U -dependent states, not like U -independent states as described earlier. The results are shown in Fig. 7 for a 8-site ring considering the effects of higher order hopping (SNH and TNH) integrals for different values of U . The kink appears for a sufficiently large value of U and its width gradually decreases as a result of higher order hopping.

■ **Configuration II – Ring with $N_{up} = 2$ and $N_{dn} = 2$:**

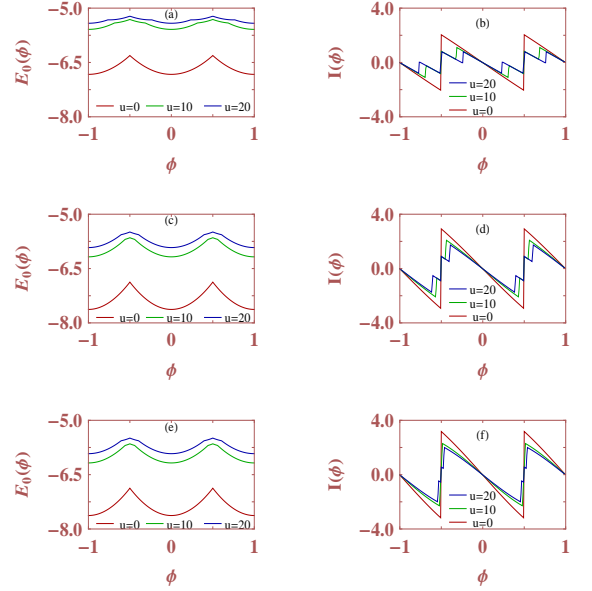


FIG. 7: (Color online). Energy and current spectra for a 8-site ring with $N_{up} = 3$ and $N_{dn} = 1$ for some typical values of U , where the first, second and third rows correspond to the ring with only NNH; NNH and SNH; NNH, SNH and TNH integrals, respectively. Here we choose $t_1 = -0.1$ and $t_2 = -0.05$.

For this configuration we choose many-body basis states as: $|\psi_1\rangle = c_{p\uparrow}^\dagger c_{q\uparrow}^\dagger c_{r\downarrow}^\dagger c_{s\downarrow}^\dagger |0\rangle$ and $|\psi_2\rangle = c_{k\uparrow}^\dagger c_{l\uparrow}^\dagger c_{m\downarrow}^\dagger c_{n\downarrow}^\dagger |0\rangle$. Here the dimension of the Hamiltonian matrix becomes $(N^2/4)(N-1)^2 \times (N^2/4)(N-1)^2$, and, it is higher compared to the Configuration I, i.e., ring with three up and one down spin electrons.

The results for a half-filled ring are displayed in Fig. 8. It is shown that in absence of electronic correlation

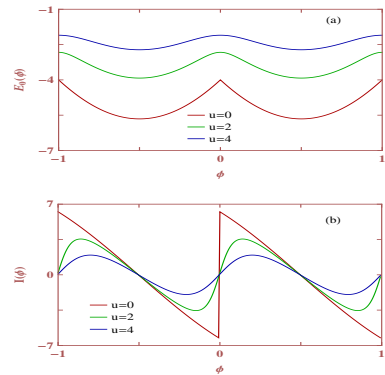


FIG. 8: (Color online). Variation of ground state energy and corresponding current for a four-site ring with $N_{up} = 2$ and $N_{dn} = 2$ for different strengths of U considering NNH only.

($U = 0$), current exhibits a sharp transition similar to that as obtained in the previous 4-electron half-filled ring, but the transition takes place at $\phi = 0$. All the other features, viz, the continuous like variation of current with

ϕ and its reduction as a result of electronic correlation remain almost similar as presented in Fig. 6. But there is a crucial difference between these two sets of electronic configurations. Comparing the current spectra given in Figs. 6(b) and 8(b) it is seen that the suppression of current due to e-e interaction becomes more significant for the ring with $N_{up} = 3$ and $N_{dn} = 1$ compared to the other case. The reason is that in the first case where $N_{up} > N_{dn}$, the hopping probability of up spin electrons is less compared to the ring with $N_{up} = N_{dn}$ since in the later case pairing of up and down spin electrons in a single site is possible as a result of hopping term for low

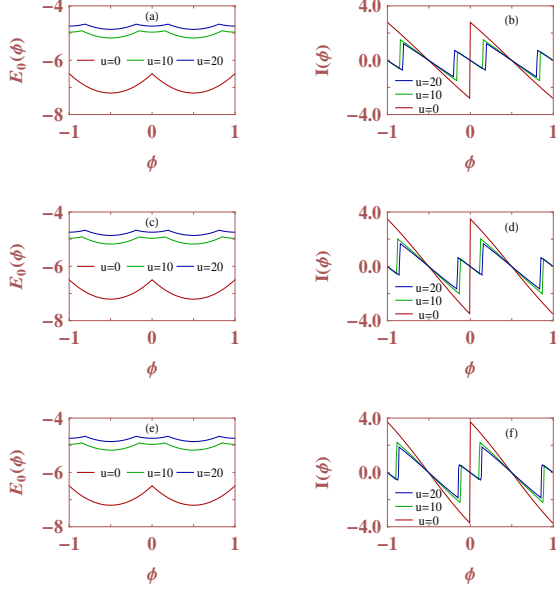


FIG. 9: (Color online). E_0 - ϕ and I - ϕ curves for a 7-site ring with $N_{up} = 2$ and $N_{dn} = 2$ for some typical values of U considering $t_1 = -0.1$ and $t_2 = -0.05$, where three different rows correspond to the identical meaning as given in Fig. 7.

U , yielding a contribution to the current. For large U in both these two cases current gets reduced.

Focusing on the spectra given in Fig. 9 apparently it seems that the features are almost identical with the results shown in Fig. 7, but there is a striking difference between the two. For this configuration ($N_{up} = N_{dn} = 2$) kink, associated with U -dependent states, appears for any non-zero correlation strength U , unlike the previous case ($N_{up} = 3$ and $N_{dn} = 1$) where a critical U (say U_c) is required. Apart from this, other qualitative features are almost identical. For all these four-electron ring systems we get only ϕ_0 periodic persistent current.

Case 4 - Ring with five electrons: Now we move to the five-electron ring system and here we also consider two distinct configurations depending on N_{up} and N_{dn} . In one configuration we set $N_{up} = 3$ and $N_{dn} = 2$, while for the other we fix $N_{up} = 4$ and $N_{dn} = 1$.

■ Configuration I – Ring with $N_{up} = 3$ and $N_{dn} = 2$:

For this configuration the many-body basis states get the forms: $|\psi_1\rangle = c_{p\uparrow}^\dagger c_{q\uparrow}^\dagger c_{r\uparrow}^\dagger c_{s\downarrow}^\dagger c_{t\downarrow}^\dagger |0\rangle$ and $|\psi_2\rangle = c_{k\uparrow}^\dagger c_{l\uparrow}^\dagger c_{m\uparrow}^\dagger c_{n\downarrow}^\dagger c_{o\downarrow}^\dagger |0\rangle$, and the dimension of the Hamiltonian for a N -site ring becomes $(N^2/12)(N-1)^2(N-2) \times (N^2/12)(N-1)^2(N-2)$.

The characteristic features of ground state energy along with persistent current for a half-filled five-electron ($N_{up} = 3$ and $N_{dn} = 2$) ring system are shown in Fig. 10.

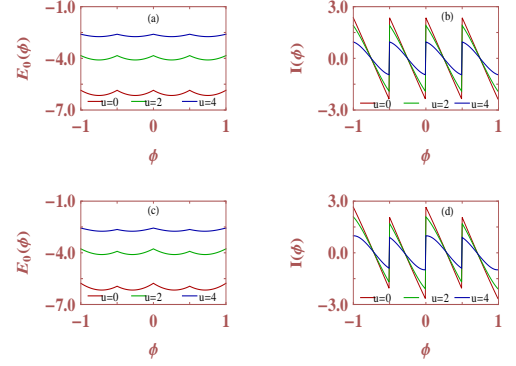


FIG. 10: (Color online). E_0 - ϕ and I - ϕ characteristics for a five-electron ($N_{up} = 3$ and $N_{dn} = 2$) half-filled ring, where the first row corresponds to the ring with only NNH integral and the second row describes the ring with NNH and SNH ($t_1 = -0.1$) integrals. Here TNH does not make any sense.

In the first row, results are given when the ring is described with only NNH, while in the other row we consider the effect of SNH integral too. For this five-site ring inclusion of TNH does not make any sense, since long-range hopping in shortest path is only the physically accessible hopping parameter. Several notable features are obtained. (i) For the ring described with only NNH, current exhibits half-flux-quantum ($\phi_0/2$) periodicity and it is not at all affected by the electronic correlation. This is exactly the same what we get in a three-electron half-filled ring (see Fig. 4). (ii) But surprisingly we see that the $\phi_0/2$ periodicity disappears when the effect of higher order hopping is included (Fig. 10(d)). From these results we can generalize that $\phi_0/2$ periodicity is specific to the odd-half-filled rings described with only NNH integral. Other properties like the reduction of current with U and the role of higher order hopping on current enhancement remain same as discussed for other cases.

The results for a five-electron ($N_{up} = 3$ and $N_{dn} = 2$) non-half-filled ring are placed in Fig. 11 considering some typical values of U . All the basic features of ground state energy and corresponding current shown in this spectra (Fig. 11) are almost similar to those given in Fig. 5 for a three-electron non-half-filled ring. For this five-electron system we can also observe kink-like structure in persistent current above a critical value of U , like the three-electron interacting ring. The critical value U_c is very large for this 7-site ring (which is not shown here in the figure) and it (U_c) becomes smaller for larger ring which we confirm through our detailed numerical calculations.

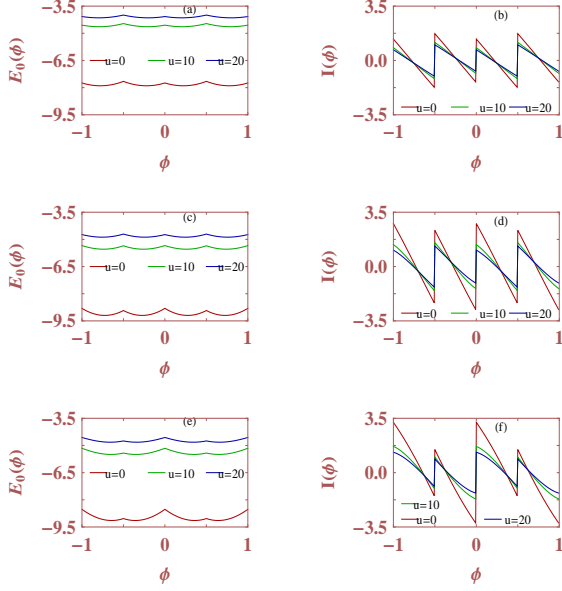


FIG. 11: (Color online). Variation of ground state energy and corresponding current for a five-electron ($N_{up} = 3$ and $N_{dn} = 2$) non-half-filled ring ($N = 7$) for some typical values of U , where the 1st, 2nd and 3rd rows represent the ring with only NNH; NNH and SNH ($t_1 = -0.4$); NNH, SNH and TNH ($t_2 = -0.2$) integrals, respectively.

The role played by higher order hopping integrals remains same as discussed in other non-half-filled rings and in all these cases current gives ϕ_0 periodicity.

■ **Configuration II – Ring with $N_{up} = 4$ and $N_{dn} = 1$:** For this set-up the basis states read as $|\psi_1\rangle = c_{p\uparrow}^\dagger c_{q\uparrow}^\dagger c_{r\uparrow}^\dagger c_{s\uparrow}^\dagger c_{t\downarrow}^\dagger |0\rangle$ and $|\psi_2\rangle = c_{k\uparrow}^\dagger c_{l\uparrow}^\dagger c_{m\uparrow}^\dagger c_{n\uparrow}^\dagger c_{o\downarrow}^\dagger |0\rangle$. Here the dimension of the Hamiltonian matrix is: $(N^2/24)(N-1)(N-2)(N-3) \times (N^2/24)(N-1)(N-2)(N-3)$ and it is less compared to the dimension of a matrix for a N -site ring having three up and two down spin electrons.

The half-flux-quantum periodicity is still preserved for a half-filled five-electron ring even when we set $N_{up} = 4$ and $N_{dn} = 1$. But the requirement is that the ring should be described with only NNH hopping, and the electronic correlation does not have any explicit dependence on it. But as long as the effect of higher order hopping is incorporated, $\phi_0/2$ periodicity gets lost and the current regains its conventional ϕ_0 periodicity. These features are clearly presented in Fig. 12 and consistent with the results shown in the spectra Fig. 10.

In the non-half-filled case some anomalous features appear in persistent current associated with ground state energy in presence of e-e interaction. The results for a seven-site ring are displayed in Fig. 13 considering $N_{up} = 4$ and $N_{dn} = 1$. For $U = 0$, sharp transitions are available, while sudden phase change in current takes place at some typical fluxes in presence of U due to U -dependent states as seen from the I - ϕ spectra. Here only

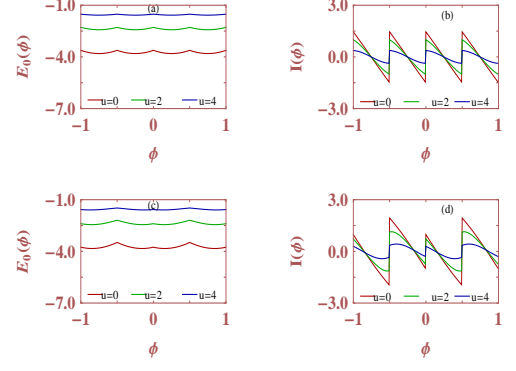


FIG. 12: (Color online). Ground state energy and corresponding current as a function of ϕ for a half-filled five-electron ring with $N_{up} = 4$ and $N_{dn} = 1$, where the top row represents the ring with NNH only, and, the bottom row describes the ring with NNH and SNH ($t_1 = -0.1$) integrals. TNH integral is redundant here.

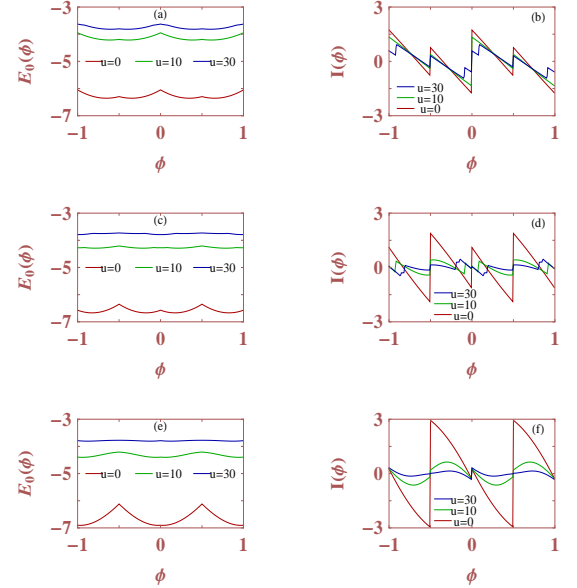


FIG. 13: (Color online). E_0 - ϕ and I - ϕ curves for a five-electron ($N_{up} = 4$ and $N_{dn} = 1$) non-half-filled ring ($N = 7$) for some particular values of U , where three different rows correspond to the identical meaning as given in Fig. 11.

ϕ_0 periodic current is obtained.

Case 5 - Ring with six electrons: Finally, we consider six-electron system to study the characteristic properties of persistent current. Depending on up and down spin electrons we focus on two distinct electronic configurations. For one configuration we set $N_{up} = N_{dn} = 3$ and for the other configuration we fix $N_{up} = 4$ and $N_{dn} = 2$.

■ **Configuration I – Ring with $N_{up} = 3$ and $N_{dn} = 3$:** The many-body basis states for this configuration look like $|\psi_1\rangle = c_{p\uparrow}^\dagger c_{q\uparrow}^\dagger c_{r\uparrow}^\dagger c_{s\downarrow}^\dagger c_{t\downarrow}^\dagger c_{u\downarrow}^\dagger |0\rangle$ and $|\psi_2\rangle =$

$c_{j\uparrow}^\dagger c_{k\uparrow}^\dagger c_{l\uparrow}^\dagger c_{m\downarrow}^\dagger c_{n\downarrow}^\dagger c_{o\downarrow}^\dagger |0\rangle$, and the dimension of the Hamiltonian matrix for a N -site ring becomes $(N^2/36)(N-1)^2(N-2)^2 \times (N^2/36)(N-1)^2(N-2)^2$.

In Fig. 14 we present the dependence of ground state energy along with persistent current for a six-site ring considering three up and three down spin electrons for

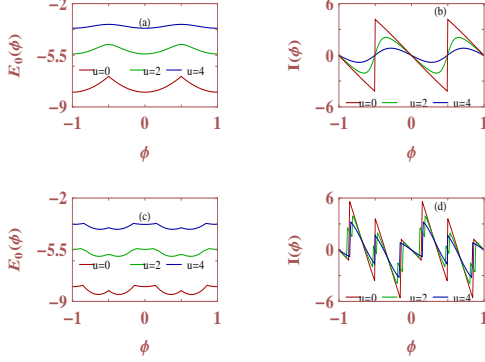


FIG. 14: (Color online). Ground state energy and current spectra for a six-site ring with three up and three down spin electrons for three distinct values of U , where the first row corresponds to the ring with only NNH and the second row represents the ring with NNH and SNH integrals. Here we set $t_1 = -0.8$.

some typical values of U . At $U = 0$ the current provides a sharp jump across $\phi = \pm\phi_0/2$, while it varies continuously with reduced amplitude in presence of finite e-e interaction. Exactly identical behavior is obtained for the four-electron half-filled ring. Thus it can be emphasized that there exists a striking similarity between all half-filled rings with even number of electrons under NNH approximation. With the addition of higher order hopping (here it is SNH), some anomalous oscillations appear as a result of phase reversal of ground state energy.

Away from half-filling kink-like structure appears following the variation of ground state energy and the width of this kink decreases with the incorporation of additional hopping integrals (see Fig. 15), similar to the four-electron ring system. In addition, current exhibits more complex structure in presence of TNH for large U .

■ Configuration II – Ring with $N_{up} = 4$ and $N_{dn} = 2$:

The basis states for this choice of up and down spin electrons are: $|\psi_1\rangle = c_{p\uparrow}^\dagger c_{q\uparrow}^\dagger c_{r\uparrow}^\dagger c_{s\uparrow}^\dagger c_{t\downarrow}^\dagger c_{u\downarrow}^\dagger |0\rangle$ and $|\psi_2\rangle = c_{j\uparrow}^\dagger c_{k\uparrow}^\dagger c_{l\uparrow}^\dagger c_{m\uparrow}^\dagger c_{n\downarrow}^\dagger c_{o\downarrow}^\dagger |0\rangle$. This configuration sets the dimension of the matrix for a N -site ring as $(N^2/48)(N-1)^2(N-2)(N-3) \times (N^2/48)(N-1)^2(N-2)(N-3)$ and it is lower than the dimension of a identical size ring containing three up and three down spin electrons.

The characteristics features of ground state energy together with persistent current for a half-filled six-electron ring with $N_{up} = 4$ and $N_{dn} = 2$ are shown in Fig. 16 for some typical values of U . Comparing the spectra given in Figs. 14 and 16 it is noticed that almost identical variation of current is obtained apart from a shifting along the

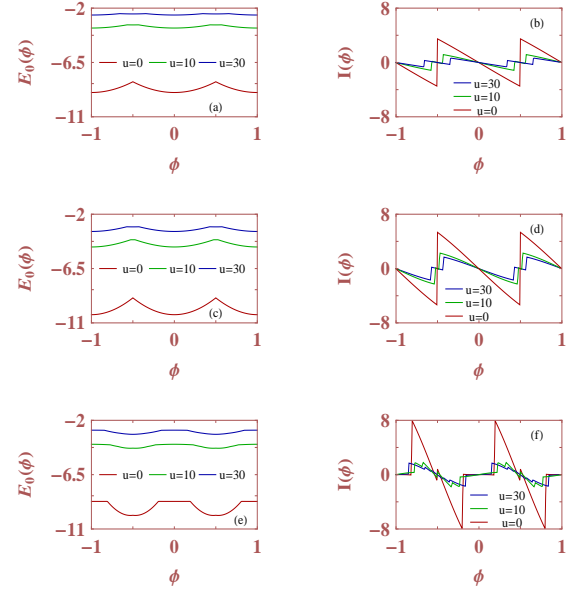


FIG. 15: (Color online). E_0 - ϕ and I - ϕ curves for a seven-site ring with three up and three down spin electrons, where the 1st, 2nd and 3rd rows correspond to the ring with only NNH; NNH and SNH ($t_1 = -0.6$); NNH, SNH and TNH ($t_2 = -0.5$) integrals, respectively.

flux line. In one case the sharp transition for $U = 0$ takes place at $\phi = \pm\phi_0/2$ (Fig. 14), while in the other case it occurs at $\phi = 0$ (Fig. 16) for the identical strength of U . These features, in fact, are quite similar to the results discussed for two different configurations in the half-filled four-electron ring system. Certainly, these observations demand that all half-filled rings with even number of electrons exhibit qualitatively identical patterns.

Quite similar argument can also be applicable for the non-half-filled case. Apart from certain kinks at dif-

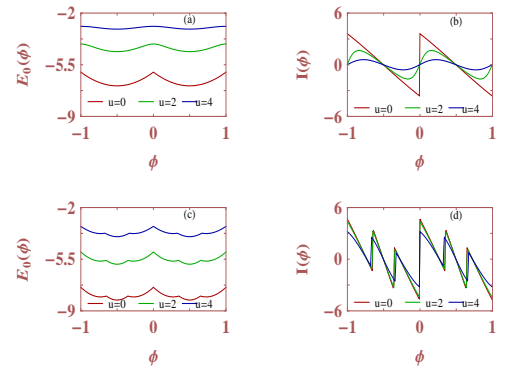


FIG. 16: (Color online). E_0 - ϕ and I - ϕ spectra for a six-site ring with $N_{up} = 4$ and $N_{dn} = 2$, where the upper and lower rows represent the similar meaning as described in Fig. 14 with identical parameter values.

ferent fluxes, current exhibit more complex structures in presence of higher order hopping as clearly seen from the

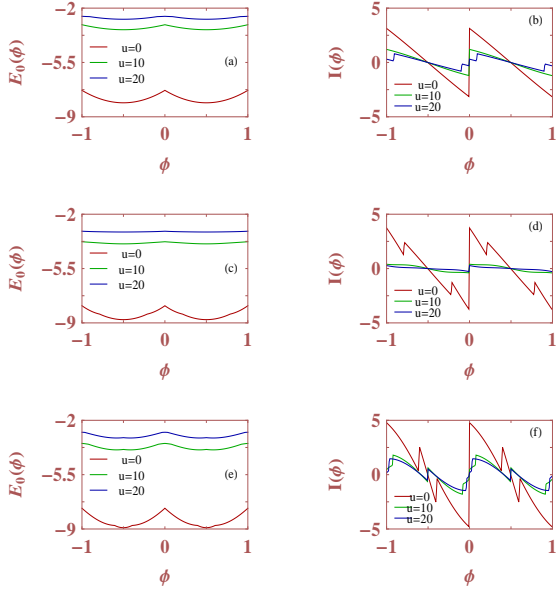


FIG. 17: (Color online). Dependence of ground state energy and associated current with flux ϕ for a seven-site ring considering $N_{up} = 4$ and $N_{dn} = 2$, where different rows correspond to the identical meaning as stated in Fig. 15. Here we set $t_1 = -0.5$ and $t_2 = -0.4$.

spectra given in Fig. 17, like the non-half-filled ring with three up and three down spin electrons (see Fig. 15). Due to smaller size of the ring (where N_e is very close to N) current gets suppressed significantly with increasing the correlation strength and this effect dominates for the maximum unequal distribution among up and down spin electrons keeping the total number of electrons constant. For all these six-electron ring systems we get only ϕ_0 periodic persistent current, like two-electron and four-electron cases.

2. Effect of impurity

Now we investigate the role of impurities on persistent current and the interplay between Hubbard interaction and long-range hopping on it. To introduce impurities in a ring we choose on-site potentials (ϵ_j) randomly from a ‘Box’ distribution function of width W setting the window region $-W/2$ to $W/2$. Since the response strongly depends on disordered configurations, we compute all the results taking average over a large number of distinct such configurations and below we present some of these essential results.

Case I - Ring with two electrons: To investigate the critical role played by disorder in Fig. 18 we display the dependence of ground state energy together with persistent current as a function of ϕ for a twenty-site ring considering two opposite spin electrons setting the disorder strength $W = 1$. In presence of disorder current

becomes vanishingly small (red curve of Fig. 18(b)) for the non-interacting ring ($U = 0$) described with NNH integral. This is solely due to electronic localization as electrons get pinned at different sites associated with the on-site potentials, and, it becomes even smaller for higher W (not shown here in the figure to save space). Now under this situation current gets enhanced if we include the effect of electronic correlation (green line of Fig. 18(b)). This correlation tries to homogenize the system providing enhanced current. But the enhancement becomes more

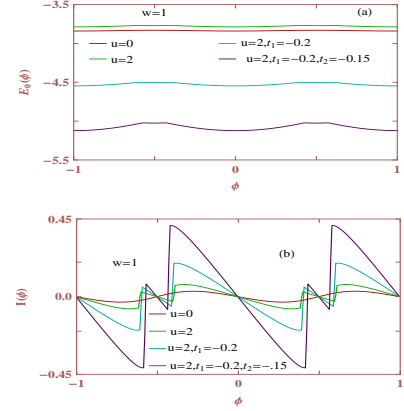


FIG. 18: (Color online). E_0 - ϕ and I - ϕ characteristics for a 20-site ring ($N = 20$) with two-opposite spin electrons in presence of disorder ($W = 1$) for some typical values U considering the effect of higher order hopping integrals.

significant when the contributions from higher order hopping integrals are taken into account. This is clearly seen from the cyan and purple curves of Fig. 18(b). Thus it can be emphasized that the effect of localization as a result of disorder in NNH model can be suppressed significantly by introducing higher order hopping integrals in presence of e-e interaction. The available current for the disordered ring in presence of higher order hopping integrals is quite comparable to the current obtained for a *perfect* non-interacting ring described with only NNH integral which, on the other hand, is very close to the experimental observations. Therefore, only NNH model is *not sufficient* to verify experimental results where the rings invariably contain disorder and certainly we have to go beyond NNH model.

Apart from this we also find that sudden phase reversal of current takes place around $\phi = \pm\phi_0/2$ due to U -independent states, like the two-electron ordered ring, but for this disordered case the kink appears beyond a critical value of U ($= U_c$, say) and it depends on ring size as well as disorder strength. Whereas, any non-zero value of U yields kink-like structure in the ordered ring. For all these cases current exhibits ϕ_0 flux-quantum periodicity.

Case II - Ring with three electrons: Finally, let us focus on the response of a three-electron disordered ring.

In Fig. 19 we present the variation of ground state energy together with persistent current for a half-filled

($N = 3$) disordered ring, described with NNH integral, considering $N_{up} = 2$ and $N_{dn} = 1$. To reveal the precise role of disorder on periodicity of ground state energy as well as current with ϕ , here we superimpose the result of an ordered interacting ring (green curve). From the spectra it is seen that $\phi_0/2$ periodicity no longer exists

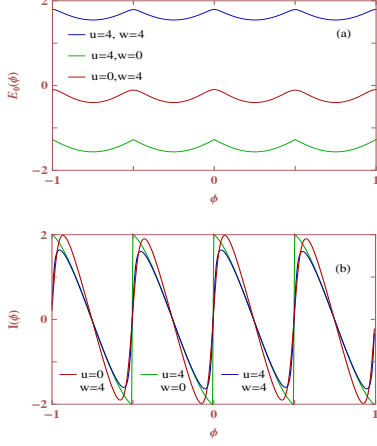


FIG. 19: (Color online). E_0 - ϕ and I - ϕ characteristics for a three-electron ($N_{up} = 2$ and $N_{dn} = 1$) ring in the half-filled case in presence of disorder. For the sake of comparison, the result of an ordered ring (green line) is also given.

in presence of disorder, and both the energy and current get usual ϕ_0 periodicity.

For this three-site ring it is quite hard to view the competition between U and W , and thus, we focus on the

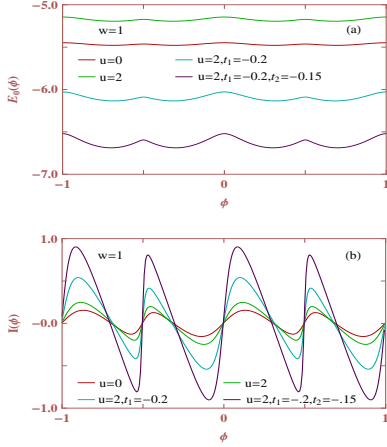


FIG. 20: (Color online). Ground state energy and corresponding current for a three-electron ($N_{up} = 2$ and $N_{dn} = 1$) ring in the non-half-filled case ($N = 10$) in presence of disorder.

spectra given in Fig. 20 where the results are shown for a ten-site ring. A significant enhancement of current takes place in presence of electronic correlation and higher order hopping integrals, and, sometimes this enhancement becomes two orders of magnitude larger compared to the NNH model.

Before we finish this sub-section we would like to point out that the characteristic features of ground state energies and corresponding persistent currents for other disordered rings with four, five and even six electrons are reviewed thoroughly and from our analysis we find exactly similar kind of enhancement and identical periodic nature of current in the presence of e-e interaction and long-range hopping.

Scaling behavior

The results analyzed so far are worked out for some typical interacting rings taking different combinations of up and down spin electrons, and, these results exhibit certain similarities among the rings with even number (two, four and six) of electrons as well as rings with odd number (three and five) of electrons. To make the analysis a self-contained one, now we discuss the dependence of current with ring size N and from it we establish its scaling behavior.

Figure 21 displays the dependence of current (I^{\max}) as a function of N considering $U = 1$ and $N_e = 2$ ($N_{up} = N_{dn} = 1$), where I^{\max} is obtained by taking the

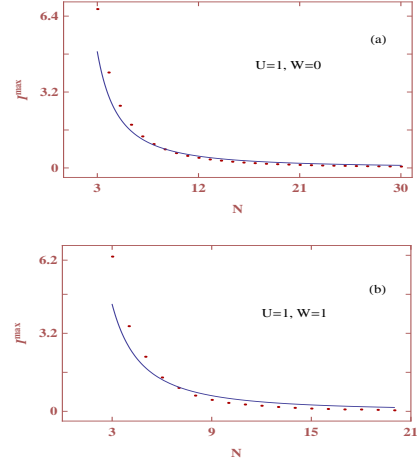


FIG. 21: (Color online). Dependence of persistent current with ring size N considering $U = 1$ and $N_e = 2$ ($N_{up} = N_{dn} = 1$). The dotted points, corresponding to the currents, are evaluated following the exact diagonalization method. Using these dots a scaling relation between the current and ring size is established which generates the continuous curve. Two cases are presented depending on W where (a) and (b) correspond to $W = 0$ and 1, respectively.

maximum absolute value of current computed within the flux range 0 to ϕ_0 . Two different cases, one is for $W = 0$ and other is for $W = 1$, are described those are given in (a) and (b), respectively. The dotted points, corresponding to current for different N , are computed following the exact diagonalization method, and, using these dots we construct a scaling behavior of current which generates the continuous line. The scaling relation gets the form: $I^{\max} = CN^{-\xi}$, where the constant C becomes 30 for both

ordered and disordered cases, while the exponent ξ becomes different in these two cases. It is 1.65 for $W = 0$ and 1.75 for $W = 1$. Usually, for a particular filling this constant (C) depends on the disorder strength, but for this typical N_e we find its identical value both for the

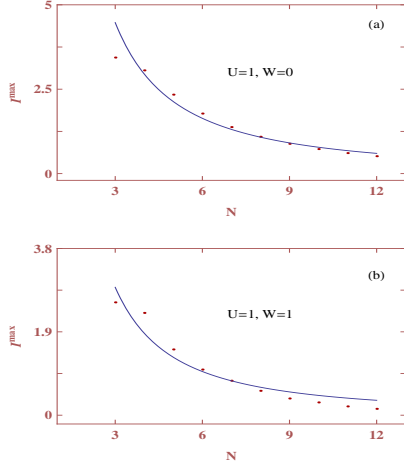


FIG. 22: (Color online). Same as Fig. 21 with $N_e = 3$, where $N_{up} = 2$ and $N_{dn} = 1$.

ordered and disordered rings which we confirm through elaborate numerical calculations.

In Fig. 22 we present the variation of current with ring size N for $N_e = 3$ (considering $N_{up} = 2$ and $N_{dn} = 1$), keeping all other physical parameters the same as taken in Fig. 22. Like two-electron system, here we also get similar kind of scaling relation, viz, $I^{\max} = CN^{-\xi}$, where the constant C becomes 22 and 16, and, the exponent ξ reaches to 1.45 and 1.55 for the ordered and disordered cases, respectively.

In the same way we can also check scaling behavior of persistent current in higher-electron systems (i.e., rings with four, five, six and more electrons), and from our analysis it can be emphasized that in each case current obeys the identical scaling relation, viz, $I \propto N^{-\xi}$. This exponent ξ gradually decreases, both for ordered and disordered cases, with N_e and for $N_e \geq 5$ it almost reaches to the limiting value 1.33 at $U = 1$, which is consistent with the previous analysis done by Gendiar *et al*³⁰ using bosonization techniques. Our analysis clearly suggests that the current decreases algebraically with ring size N .

B. Hartree-Fock mean field analysis

In this sub-section we present numerical results computed from HF mean-field approach and compare these results with those obtained from the other method i.e., exact numerical diagonalization.

Figure 23 displays the dependence of ground state energy together with persistent current as a function of flux ϕ for some typical ordered rings (even N) described with

only NNH integral in the limit of half-filling considering different values of electronic correlation strength U . Two cases are analyzed depending on the ring size N . In the first row we present the results for $N = 6$ and $N_{up} = N_{dn} = 3$, to compare these spectra with our previous data (top row of Fig. 14) obtained from exact

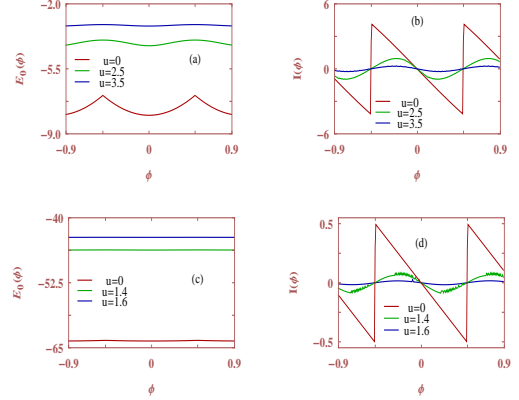


FIG. 23: (Color online). Dependence of ground state energy and corresponding persistent current as a function of ϕ for some typical ordered rings, described with only NNH integral, in the half-filled band case considering different values of U . In the first row we choose $N = 6$ and $N_{up} = N_{dn} = 3$, while in the second row these parameters are: $N = 50$ and $N_{up} = N_{dn} = 25$.

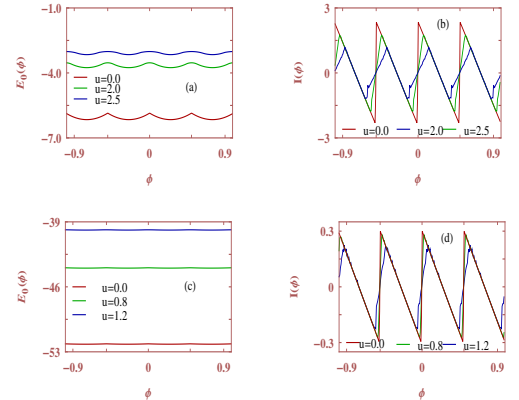


FIG. 24: (Color online). E_0 - ϕ and I - ϕ spectra for some typical ordered rings, described with only NNH integral, in the half-filled band case considering different values of U . In the first row we choose $N = 5$, $N_{up} = 3$ and $N_{dn} = 2$, while in the second row these parameters are: $N = 41$, $N_{up} = 21$ and $N_{dn} = 20$.

numerical diagonalization method. Comparing the spectra Figs. 23(b) and 14(b) we see that MF results are highly consistent with our data obtained from exact numerical diagonalization of the many-body Hamiltonian. Therefore, we can certainly rely on MF solutions and extend our analysis to larger rings. As illustrative example, in the second row of Fig. 23 we present the MF results

for a 50-site ring, and they exhibit almost identical features, like a 6-site ring, which yield the invariant nature of energy- and current-flux characteristics for different ring sizes when the filling factor remains constant.

In a similar way we now focus our attention on the rings with odd N . The results are shown in Fig. 24 where we present the behavior of ground state energy and corresponding persistent current, obtained from MF technique, for two different ring sizes. The spectra for $N = 5$ (first row of Fig. 24) can be directly compared to the results given in the first row of Fig. 10 since all the physical parameters are same for these two cases. Quite interestingly we see that almost all the features, viz, suppression of current with U and half flux-quantum periodicity as a function of ϕ remain unchanged. But, for narrow regions of ϕ the slope of the currents for non-zero U shows opposite signature in these two different numerical methods, while it (slope) remains same for other flux

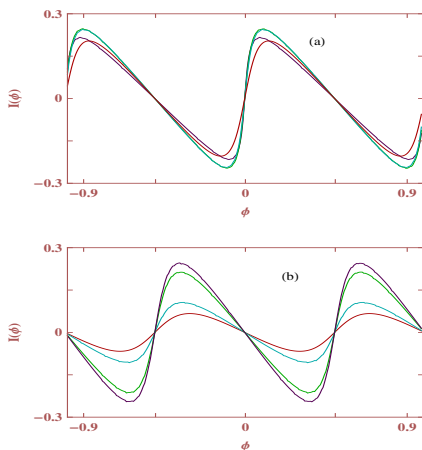


FIG. 25: (Color online). Variation of persistent current for a 60-site disordered ($W = 1$) ring, where (a) $N_{up} = N_{dn} = 30$ and (b) $N_{up} = N_{dn} = 15$. The red line corresponds to the disordered non-interacting ($U = 0$) ring with only NNH integral, while introducing the effect of e-e interaction ($U = 0.5$) in this ring we get cyan curve. The green curve represents the ring with disorder, e-e interaction ($U = 0.5$) and SNH integral ($t_1 = -0.2$), whereas the purple line corresponds to the ring with disorder, e-e interaction ($U = 0.5$), SNH ($t_1 = -0.2$) and TNH ($t_2 = -0.05$) integrals.

regions. This is the peculiarity of MF calculations and can be noticed for any other ordered rings with odd N in the limit of half-filling. To substantiate it in the second row of Fig. 24 we present the results for a 41-site ring considering $N_{up} = 21$ and $N_{dn} = 20$, and see that all the properties exhibited by a 5-site ring are nicely followed in this bigger ring.

Finally, let us focus on the MF results given in Fig. 25

where we present the variation of persistent current for a 60-site ring as a function of ϕ considering two different band fillings those are placed in (a) and (b), respectively. Four distinct cases are analyzed depending on the physical parameters of the system. The red curve corresponds to the current for the non-interacting ($U = 0$) disordered ($W = 1$) ring described with only NNH integral. While introducing the effect of e-e interaction in this ring we get cyan curve. The green line represents the current for the ring with disorder, e-e interaction and SNH integral, whereas incorporating further the effect of TNH integral in this ring we get the current shown by the purple curve. At half-filling all the currents are quite comparable with each other (Fig. 25(a)) and higher order hopping integrals do not actually play any such significant role in enhancing the current since it is counterbalanced by the repulsive Coulomb interaction. On the other hand, at less than half-filling an enhancement of current takes place as a result of U and it becomes more significant in presence of higher order hopping integrals (Fig. 25(b)) as there exists empty sites where electrons can hop quite easily yielding more current. These mean-field results are fully consistent with our exact numerical diagonalization analysis (see Figs. 19 and 20).

IV. CLOSING REMARKS

To conclude, in this work we have investigated the behavior of ground state energy and persistent current in interacting mesoscopic rings subjected to AB flux ϕ in presence of long-range hopping and disorder. Two different methods, exact numerical diagonalization and HF mean-field theory, have been used to compute numerical results of the many-body systems, and, found that the results obtained from these two methods are highly consistent with each other. The interplay between Hubbard interaction and long-range hopping integrals yields a significant enhancement of persistent current in disordered ring which in some cases becomes comparable to that of an ordered ring and reaches very close to the experimental observations. This phenomenon suggests that only e-e interaction is not sufficient to explain the enhancement of persistent current in a disordered ring described with NNH integral. We have to incorporate the effect of higher order hopping integrals. From our results we have shown that even for too small values of t_1 and t_2 compared to t , current gets enhanced significantly. In addition, we have also discussed the appearance of $\phi_0/2$ periodic current for some typical electron fillings and its sensitivity on higher order hopping as well as randomness. Finally, we have analyzed the scaling behavior of current which suggests an asymptotic decay with ring size N .

* Electronic address: madhumitasaha91@gmail.com

† Electronic address: santanu.maiti@isical.ac.in

- ¹ M. Büttiker, Y. Imry, and R. Landauer, Phys. Lett. A **96**, 365 (1983).
- ² Y. Imry, *Introduction to mesoscopic physics*, Oxford University Press, Oxford (1997).
- ³ L. P. Lévy, G. Dolan, J. Dunsmuir, and H. Bouchiat, Phys. Rev. Lett. **64**, 2074 (1990).
- ⁴ E. M. Q. Jariwala, P. Mohanty, M. B. Ketchen, and R. A. Webb, Phys. Rev. Lett. **86**, 1594 (2001).
- ⁵ N. O. Birge, Science **326**, 244 (2009).
- ⁶ V. Chandrasekhar, R. A. Webb, M. J. Brady, M. B. Ketchen, W. J. Gallagher, and A. Kleinsasser, Phys. Rev. Lett. **67**, 3578
- ⁷ W. Rabaud, L. Saminadayar, D. Mailly, K. Hasselbach, A. Benoit, and B. Etienne, Phys. Rev. Lett. **86**, 3124 (2001).
- ⁸ D. Mailly, C. Chapelier, and A. Benoit, Phys. Rev. Lett. **70**, 2020 (1993).
- ⁹ H. Bluhm, N. C. Koshnick, J. A. Bert, M. E. Huber, and K. A. Moler, Phys. Rev. Lett. **102**, 136802 (2009).
- ¹⁰ H. F. Cheung, Y. Gefen, E. K. Reidel, and W. H. Shih, Phys. Rev. B **37**, 6050 (1988).
- ¹¹ N. Bayers and C. N. Yang, Phys. Rev. Lett. **7**, 46 (1961).
- ¹² H. F. Cheung, E. K. Riedel, and Y. Gefen, Phys. Rev. Lett. **62**, 587 (1989).
- ¹³ G. Montambaux, H. Bouchiat, D. Sigeti, and R. Friesner, Phys. Rev. B **42**, 7647 (1990).
- ¹⁴ G. Bouzerar, D. Poilblanc, and G. Montambaux, Phys. Rev. B **49**, 8258 (1994).
- ¹⁵ T. Giamarchi and B. S. Shastry, Phys. Rev. B **51**, 10915 (1995).
- ¹⁶ S. K. Maiti, J. Chowdhury and S. N. Karmakar, Phys. Lett. A **332**, 497 (2004).
- ¹⁷ S. K. Maiti, Solid State Phenomena **155**, 87 (2009).
- ¹⁸ M. Saha and S. K. Maiti, Physics Letters A **380**, 1450 (2016).
- ¹⁹ V. Ambegaokar and U. Eckern, Phys. Rev. Lett. **65**, 381 (1990).
- ²⁰ A. Schmid, Phys. Rev. Lett. **66**, 80 (1991).
- ²¹ U. Eckern and A. Schmid, Europhys. Lett. **18**, 457 (1992).
- ²² H. Bary-Soroker, O. Entin-Wohlman, and Y. Imry, Phys. Rev. B **82**, 144202 (2010).
- ²³ B. Reulet, M. Ramin, H. Bouchiat, and D. Mailly, Phys. Rev. Lett. **75**, 124 (1995).
- ²⁴ S. K. Maiti, J. Chowdhury, and S. N. karmakar, J. Phys.: Condens. Matter **18**, 5349 (2006).
- ²⁵ S. K. Maiti, Int. J. Mod. Phys. B **21**, 179 (2007).
- ²⁶ H. Kato and D. Yoshioka, Phys. Rev. B **50**, 4943 (1994).
- ²⁷ A. Kambili, C. J. Lambert, and J. H. Jefferson, Phys. Rev. B **60**, 7684 (1999).
- ²⁸ S. Gupta, S. Sil, and B. Bhattacharyya, Physica B **355**, 299 (2005).
- ²⁹ S. K. Maiti and A. Chakrabarti, Phys. Rev. B **82**, 184201 (2010).
- ³⁰ A. Gendiar, R. Krcmar, and M. Weyrauch, Phys. Rev. B **79**, 205118 (2009).